

Investigation of the elastic and photoelastic properties and refractive index of TbF₃

E. Käräjämäki, R. Laiho, and T. Levola

Wihuri Physical Laboratory, University of Turku, 20500 Turku 50, Finland

(Received 3 December 1980)

Brillouin scattering of light from the acoustic phonons in TbF₃ was investigated over a large temperature range. Values of the elastic and photoelastic coefficients and of Debye $\Theta = 373$ K were calculated from data obtained at 300 K. The temperature dependence of scattering from the longitudinal phonons propagating along [010], [001], and [011] revealed an elastic anomaly of the lattice at about 180 K. In connection with these measurements the values and dispersions of the refractive indices were also measured.

I. INTRODUCTION

A number of crystals with a high concentration of rare-earth ions have interesting magnetic phase transitions and lattice deformations. Since the absorption and emission lines of rare-earth ions are usually narrow in a crystalline environment, they have received much attention as objects for crystal-field investigations. In addition, methods of optical spectroscopy can often provide accurate information on local magnetic interactions. Part of the spectroscopic work has been carried out with emphasis on developing small-size crystal lasers by using a high concentration of active ions. For the above reasons attention has also been paid to TbF₃, which is a transparent low-temperature ferromagnet with predominantly dipolar coupling.

The basic magnetic properties^{1,2} as well as the optical absorption and emission spectra^{3,4} of TbF₃ have been investigated. The room-temperature structure of TbF₃ is orthorhombic⁵ D_{2h}^{16} - $Pnma$. As is common to many other rare-earth trifluorides this crystal has a polymorphic phase transition around 950 °C.⁶ However, the information about the lattice properties of TbF₃ at lower temperatures is rather limited. We report here the results of our Brillouin scattering investigation of acoustic phonons in TbF₃. From the data obtained values of the elastic and photoelastic coefficients were calculated. The behavior of different phonon modes was measured over a large temperature range in order to detect possible lattice deformations. Values of the refractive indices and their dispersions were also determined.

II. EXPERIMENTAL PROCEDURE

The sample crystals were oriented to an accuracy of $\pm 2^\circ$ by using the Laue back-reflection method. After cutting and polishing, the sizes of the samples were typically $4 \times 4 \times 4$ mm³. For measurements of the refractive indices, two prisms with the refractive edges along the a and

c axes and with respective refractive angles of 25.88° and 25.74° were prepared. Measurements were made by using a goniometer and six wavelengths of a Kr-ion laser.

For the Brillouin scattering investigations, the 530.9-nm line of the laser was selected. Around this wavelength the crystal has no absorption lines of the Tb³⁺ ions,³ and the fluorescence caused by the exciting light is comparatively weak. Single-mode operation of the laser was achieved by using an intracavity etalon. The spectrum of the scattered light was analyzed with the aid of a three-pass Fabry-Perot interferometer whose free spectral range was calibrated to the accuracy better than 0.1%. In order to determine values of the photoelastic coefficients, the intensities of the components of the scattering spectrum were measured. This was done by integrating over the spectral components displayed on the screen of a multi-channel analyzer used to collect the data. After that the background was subtracted. For the intensity measurements, the interferometer was used as a five-pass version resulting in the reduction of the background by more than 3 orders of magnitude. The low-temperature measurements were made with the crystal in the exchange chamber of an optical Dewar. Care was taken to minimize the heating of the sample by the laser beam.

III. BRILLOUIN SCATTERING RESULTS

The momentum conservation in the inelastic scattering of light from phonons can be written as

$$\vec{k}_s = \vec{k}_i + \vec{q}, \quad (1)$$

where \vec{k}_s , \vec{k}_i , and \vec{q} are the wave vectors of scattered light, incident light, and acoustic wave. Starting from Eq. (1) and taking account of the conservation of energy in the scattering process, the Brillouin shifts $\Delta\nu$ can be given in the form

$$\Delta\nu = \frac{v}{\lambda} (n_i^2 + n_s^2 - 2n_i n_s \cos\phi)^{1/2}, \quad (2)$$

TABLE I. Examples of the Brillouin measurements. The polarizations of the incident and the scattered light are indicated by e_i and e_s , respectively. The values of $\Delta\nu$ are given for $\lambda = 530.9$ nm and $T = 300$ K. L , T , and M represent the longitudinal, transverse, and mixed v phonon modes.

q	k_i	k_s	e_i	e_s	Mode	$\Delta\nu$ (GHz)	v (m/s)	γ
100	-100	100	010	010	L	32.78	5472	C_{11}
010	0-10	010	100	100	L	34.49	5704	C_{22}
001	00-1	001	100	100	L	26.84	4439	C_{33}
110	-1-10	110	001	001	L	32.40	5470	γ^{10^a}
110	-1-10	110	001	1-10	T	17.54	2937	$(C_{44} + C_{55})/2$
011	0-10	001	001	100	T	11.60	2742	$(C_{55} + C_{66})/2$
011	0-1-1	011	100	100	L	30.29	5009	γ^{13^b}
011	0-1-1	011	100	100	M	17.24	2851	γ^{14^c}
101	-100	001	010	010	L	23.21	5479	γ^{16^d}

$$^a \gamma^{10} = \frac{1}{4} \{ C_{11} + C_{22} + 2C_{66} + [(C_{11} - C_{22})^2 + 4(C_{12} + C_{66})^2]^{1/2} \}.$$

$$^b \gamma^{13} = \frac{1}{4} \{ C_{22} + C_{33} + 2C_{44} + [(C_{22} - C_{33})^2 + 4(C_{23} + C_{44})^2]^{1/2} \}.$$

$$^c \gamma^{14} = \frac{1}{4} \{ C_{22} + C_{33} + 2C_{44} - [(C_{22} - C_{33})^2 + 4(C_{23} + C_{44})^2]^{1/2} \}.$$

$$^d \gamma^{16} = \frac{1}{4} \{ C_{11} + C_{33} + 2C_{55} + [(C_{33} - C_{11})^2 + 4(C_{13} + C_{55})^2]^{1/2} \}.$$

where v is the velocity of the acoustic wave and λ is the wavelength of incident light. The refractive indices n_i and n_s are defined for the directions of the incident and scattered light propagating with the mutual angle ϕ . Employing both right-angle and backscattering geometries,⁷ altogether twenty scattering cases were analyzed, nine of which are

included in Table I. The values of $n_a = 1.605$, $n_b = 1.590$, and $n_c = 1.572$ were used to calculate the velocities of the different phonon modes.

Figure 1 shows the temperature dependences of $\Delta\nu$ for the longitudinal-phonon modes propagating along the axes of the crystal. It is evident that a slight change of the velocity of phonons with q parallel to $[100]$ takes place at about 400 K. Presumably this change can be connected with some type of diffusional motion causing the broadening and gradual disappearance of the ^{19}F nuclear magnetic resonance lines in TbF_3 in the same temperature region.⁸ More pronounced changes can be

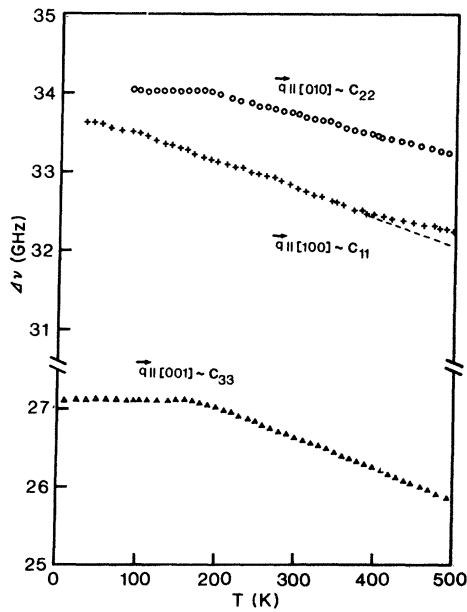


FIG. 1. Temperature dependences of the Brillouin shifts for longitudinal phonons propagating along the three principal directions of a TbF_3 crystal. The measurements were made in the backscattering geometry.

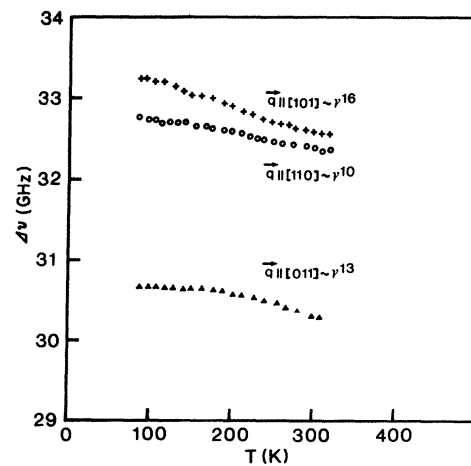


FIG. 2. Temperature dependences of the Brillouin shifts for longitudinal phonons propagating in the directions between the principal axes. The measurements were made in the backscattering geometry.

seen around 180 K in the velocities of the longitudinal phonons propagating along [010] or [001]. A similar change also takes place when the wave-vector of the longitudinal phonon is directed along [011] (see Fig. 2). Backscattering along [001] and [100] was strong enough to allow measurements down to 7 K. Below that temperature the intensity became so weak that it was not possible to investigate the behavior of phonons around the magnetic phase transition point $T_c = 3.9$ K. Application of a magnetic field at higher temperatures was not found to produce any measurable changes in the frequencies of the Brillouin lines.

A. The elastic coefficients

The components of the displacement U of a volume element of matter with density ρ are connected to the elements C_{ijkl} of the elastic stiffness tensor by the differential equation

$$\rho U_i = C_{ijkl} \frac{\partial^2 U_l}{\partial x_j \partial x_k} \quad (3)$$

By using the plane-wave solution Eq. (3) becomes

$$\gamma U_i = C_{ijkl} q_j q_k U_l \quad (4)$$

with $\gamma = \rho v^2$. The direction cosine of the unit vector perpendicular to the wave plane is indicated by q_ν . Three real solutions for γ can be obtained by solving the determinantal equation

$$\det |C_{ijkl} q_j q_k - \delta_{ij} \gamma| = 0. \quad (5)$$

Some examples of the combinations of C_{ijkl} appropriate to the crystal symmetry of TbF_3 and to the scattering geometries used are given in Table I, where the usual short-hand notation 11-1, 22-2, 33-3, 23, 32-4, 31, 13-5, 12, 21-6 has been applied. The value of $\rho = 7236 \text{ kg/m}^3$ was used to calculate C_{ij} . The results are given in Table II.

The main errors arise from the drift, nonlinearity, and calibration errors of the interferometer, from the misalignment of the light beams inside the sample, and from inaccuracies of the mass density and the refractive indices. In most cases the upper limits of the errors caused by these factors can be determined by repeated experiments. Altogether 20 scattering cases were analyzed. Hence, 11 cases could be used for cross checking of the data. The consistency of the velocity of the longitudinal phonons was found to be better than 0.5%. However, rather large uncertainty must be tolerated for those C_{ij} calculated from a complex set of coefficients in γ . From the above results for C_{ij} a value of 373 K was calculated for the Debye Θ at 300 K.

TABLE II. Values of the elastic coefficients of TbF_3 in units of 10^{10} N/m^2 .

C_{ij}	$T = 300 \text{ K}$	$T = 90 \text{ K}$
C_{11}	21.52 ± 0.20	22.63 ± 0.20
C_{22}	23.49 ± 0.20	23.91 ± 0.20
C_{33}	14.28 ± 0.20	14.83 ± 0.20
C_{44}	5.16 ± 0.50	
C_{55}	6.71 ± 0.50	
C_{66}	4.17 ± 0.50	
C_{12}	12.43 ± 2.00	
C_{13}	11.14 ± 0.60	
C_{23}	6.22 ± 1.00	

B. The photoelastic coefficients

The intensity of Brillouin scattering is proportional to the square of the combination of the photoelastic coefficients p_{ij} determined by the symmetry group of the sample crystal and the experimental geometry.⁷ When the incident and scattered light in the crystal are polarized as \vec{e}_i and \vec{e}_s , and the corresponding refractive indices are n_i and n_s , the scattered intensity can be given as^{9, 10}

$$I_{is} \sim \frac{8\pi^2 kT}{\lambda^4} \frac{(n_\nu^2 n_\mu^2 e_{s\nu} p'_{\nu\mu ki} v_k q_i e_{i\mu})^2}{(n_i + 1)^2 (n_s + 1)^2 \rho v_{is}^2} \quad (6)$$

for a unit solid angle calculated externally to the crystal. The symbols n_ν and n_μ refer to the principal refractive indices and $e_{i\nu}$ and $e_{s\mu}$ are the ν th and μ th components of the vectors \vec{e}_i and \vec{e}_s . The direction cosine of the displacement vector of the phonon propagating into the direction \vec{q}_i is given by v_k and its velocity by v_{is} . Formula (6) includes the correction for reflection of light from the front and back surface of the crystal.

The absolute values of the photoelastic coefficients were determined by comparison with the scattering intensity from fused SiO_2 for which the values of p_{ij} (Refs. 11 and 12) and C_{ij} are known. The dependence of the efficiency of the measuring set-up was determined for the different scattering cases and applied to the results. Because TbF_3 is free of absorption bands around the measuring wavelength 530.9 nm, the errors due to transmission losses and multiple internal reflections were assumed to be negligible as compared with those due to the fluctuation of the laser power and other errors of instrumental origin. Altogether 36 scattering cases were used in the intensity measurements for confirmation of both the signs and the absolute values of the photoelastic coefficients. The results are compiled in Table III.

In order to take account of the roto-optic effect,¹³ the photoelastic tensor components of a birefringent crystal must be given in the form

TABLE III. Photoelastic coefficients of TbF_3 at $\lambda = 530.9$ nm and $T = 300$ K.

p_{ij}		p'_{ij}	
p_{11}	0.218 ± 0.040	p'_{44}	-0.026
p_{22}	0.190 ± 0.040	p'_{44}	-0.035
p_{33}	0.261 ± 0.040	p'_{55}	0.017
p_{44}	-0.031 ± 0.006	p'_{55}	0.033
p_{55}	0.025 ± 0.005	p'_{66}	-0.021
p_{66}	-0.025 ± 0.005	p'_{66}	-0.029
p_{12}	0.109 ± 0.020	$p'_{44} = p_{44} + 0.0046$	
p_{21}	0.137 ± 0.020	$p'_{44} = p_{44} - 0.0046$	
p_{13}	0.127 ± 0.020	$p'_{55} = p_{55} + 0.0082$	
p_{31}	0.160 ± 0.030	$p'_{55} = p_{55} - 0.0082$	
p_{23}	0.181 ± 0.040	$p'_{66} = p_{66} + 0.0037$	
p_{32}	0.152 ± 0.030	$p'_{66} = p_{66} - 0.0037$	

$$p'_{ijkl} = p_{ijkl} + \frac{1}{2} (n_i^{-2} - n_j^{-2}) (\delta_{il} \delta_{kj} - \delta_{ik} \delta_{lj}), \quad (7)$$

where p_{ijkl} is a component of the Pockel's tensor. Those values of p'_{ijkl} which differ from p_{ij} are included in Table III. It is evident that the roto-optic effect has a measurable contribution to the photoelastic properties of TbF_3 .

IV. THE REFRACTIVE INDICES

To calculate the values of the elastic coefficients from Brillouin data the refractive indices of the crystal must be known. Because these were not readily available for TbF_3 (Ref. 14) they were determined by using the two prisms as described in Sec. II. The results are quoted for $\lambda = 530.9$ nm in Table IV. Also the dispersions of the refractive indices were investigated at six wavelengths of the Kr-ion laser. From the various dispersion formulas available, the single-oscillator-type equation¹⁵

$$n^2 - 1 = \frac{E_0 E_d}{E_0^2 - \hbar^2 \omega^2} \quad (8)$$

was fitted with the experimental data. This formula has a rather straightforward connection with the ionic parameters: E_0 is the energy of the oscillator and E_d is the dispersion energy which is taken as a measure of the interband transitions. The dispersion curves are illustrated in Fig. 3.

For a number of ionic compounds the quantity $\beta = E_d / N_c Z_a N_e$ is known to be 0.26 ± 0.04 eV. Here, N_c is the coordination number of the cation near-

TABLE IV. The values of the refractive indices for $\lambda = 530.9$ nm and the dispersion parameters of TbF_3 at 300 K.

	$n_a = 1.605$	$n_b = 1.590$	$n_c = 1.572$
E_0	14.5 eV	14.6 eV	14.8 eV
E_d	22.3 eV	21.7 eV	20.8 eV

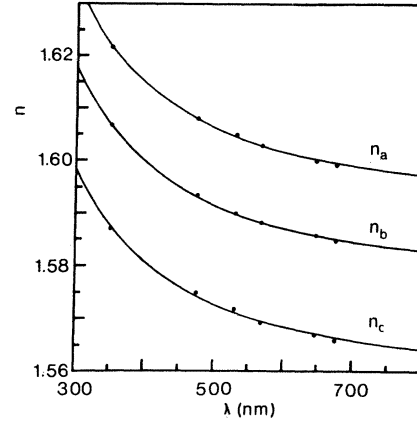


FIG. 3. Dispersions of the refractive indices of TbF_3 at 300 K. The solid lines represent the fits of Eq. (8) to the experimental points.

est neighbor, Z_a is the formal chemical valency of the anion, and N_c is the effective number of the valence electrons of the anion. For TbF_3 we get $\beta = 0.30$. The dispersion parameter E_d is somewhat greater than is usual in the simple halide crystals like alkali halides.

V. CONCLUSIONS

Brillouin scattering spectroscopy is becoming a unique method of investigating the elastic and photoelastic properties of crystals. Especially the measurements of crystals with low symmetry and reduced size are considerably easier to perform than by the usual ultrasonic methods. With a carefully constructed spectrometer it is often possible to determine the frequencies of the acoustic phonons down to liquid-nitrogen and even to liquid-helium temperatures.

According to the present results the elastic coefficients of TbF_3 are rather high and thereby reflect the good mechanical properties of the crystal. The interatomic forces appear to be larger in the ab plane than in the direction of the c axis, which can be seen from the ratios of the elastic coefficients $C_{11}/C_{33} \approx C_{22}/C_{33} \approx 1.5$. Instead, the values of the photoelastic coefficients are not very large when compared with those of fused silica and other materials applied as components for photoelastic modulators.

Small lattice anomalies were found from the temperature dependence of the longitudinal phonons propagating in the direction of the crystal axes. It is likely that the small change of the velocity of phonons propagating along $[100]$ at 400 K has some connection with the diffusional motion observed earlier by NMR spectroscopy.⁸ The more pronounced changes at 180 K in the velocities of phonons propagating in the directions $[010]$, $[001]$, and $[011]$ suggest a lattice instability at that tem-

perature. It is possible that a long precursor softening of the elastic coefficients can be seen in crystals which have a magnetic phase transition.¹⁶ In the present crystal the magnetic interactions are due to dipole-dipole coupling, and it is not clear that they have a significant contribution to the observed lattice anomaly. As can be seen from Fig. 1, C_{11} and C_{22} are clearly different at high temperatures but almost coincide close to the magnetic-phase-transition point. Thus the symmetry of the interatomic forces approaches the tetragonal limit at low temperatures. Further investigations by different methods are needed to confirm

these findings and to clarify their origin in detail.

The currently available information about the lattice dynamics of rare-earth trifluorides is still rather meager. Our results for TbF_3 suggest that investigations into the properties of phonons should be made also in the other crystals belonging to the same group.

ACKNOWLEDGMENTS

The authors wish to thank the Wihuri foundation for financial support and Mr. M. Robinson for the high-quality single crystals.

¹L. Holmes, H. J. Guggenheim, and G. W. Hull, *Solid State Commun.* **8**, 2005 (1970).

²J. Brinkmann, R. Courths, S. Hufner, and H. J. Guggenheim, *J. Magn. Magn. Mater.* **6**, 279 (1977).

³D. C. Krupka and H. J. Guggenheim, *J. Chem. Phys.* **51**, 4006 (1969).

⁴L. A. Bumagina, B. N. Kazakov, B. Z. Malkin, and A. L. Stolov, *Fiz. Tverd. Tela (Leningrad)* **19**, 1073 (1977) [*Sov. Phys.—Solid State* **19**, 624 (1977)].

⁵A. Zalkin and D. H. Templeton, *J. Am. Chem. Soc.* **75**, 2453 (1953).

⁶B. P. Sobolev, P. P. Fedorov, D. B. Shteynberg, B. V. Sinitsyn, and G. S. Shakhkalamian, *J. Solid State Chem.* **17**, 191 (1976), and references therein.

⁷R. Vacher and L. Boyer, *Phys. Rev. B* **6**, 369 (1972).

⁸A. Reuveni and B. R. McGarvey, *J. Magn. Reson.* **29**, 21 (1978).

⁹G. B. Benedek and K. Fritsch, *Phys. Rev.* **149**, 647 (1966).

¹⁰D. F. Nelson and P. D. Lazay, *Phys. Rev. B* **6**, 3109 (1972).

¹¹W. Primak and D. Post, *J. Appl. Phys.* **30**, 779 (1959).

¹²R. M. Waxler, D. Horowitz, and A. Feldman, *Appl. Opt.* **16**, 20 (1977).

¹³D. F. Nelson and M. Lax, *Phys. Rev. B* **3**, 2778 (1971).

¹⁴R. E. Thoma and D. Brunton, *Inorg. Chem.* **5**, 1937 (1966).

¹⁵S. H. Wemple and M. Di Domenico, Jr., *Phys. Rev. B* **3**, 1338 (1971).

¹⁶A. Yu Wu, *Phys. Rev. B* **13**, 4857 (1976).